

Dendritic Chelating Agents. 1. Cu(II) Binding to Ethylene Diamine Core Poly(amidoamine) Dendrimers in Aqueous Solutions

Mamadou S. Diallo,^{*,†,‡} Simone Christie,[‡] Pirabalini Swaminathan,[‡]
Lajos Balogh,[§] Xiangyang Shi,[§] Wooyong Um,^{||} Charalambos Pangelis,[⊥]
William A. Goddard III,[†] and James H. Johnson, Jr.[‡]

Materials and Process Simulation Center, Beckman Institute, California Institute of Technology, Pasadena, California 91125, Department of Civil Engineering, Howard University, Washington, D.C. 20059, Center for Biologic Nanotechnology, University of Michigan, Ann Arbor, Michigan 48109-0533, Applied Geology and Geochemistry, Pacific Northwest National Laboratory, Richland, Washington 99352, and Division of Hydrologic Sciences, Desert Research Institute, University of Nevada System, Las Vegas, Nevada 89119

Received November 9, 2003. In Final Form: January 22, 2004

This paper describes an investigation of the uptake of Cu(II) by poly(amidoamine) (PAMAM) dendrimers with an ethylenediamine (EDA) core in aqueous solutions. We use bench scale measurements of proton and metal ion binding to assess the effects of (i) metal ion–dendrimer loading, (ii) dendrimer generation/terminal group chemistry, and (iii) solution pH on the extent of binding of Cu(II) in aqueous solutions of EDA core PAMAM dendrimers with primary amine, succinamic acid, glycidol, and acetamide terminal groups. We employ extended X-ray absorption fine structure (EXAFS) spectroscopy to probe the structures of Cu(II) complexes with G_x-NH₂ EDA core PAMAM dendrimers in aqueous solutions at pH 7.0. The overall results of the proton and metal ion binding measurements suggest that the uptake of Cu(II) by EDA core PAMAM dendrimers involves both the dendrimer tertiary amine and terminal groups. However, the extents of protonation of these groups control the ability of the dendrimers to bind Cu(II). Analysis of the EXAFS spectra suggests that Cu(II) forms octahedral complexes involving the tertiary amine groups of G_x-NH₂ EDA core PAMAM dendrimers at pH 7.0. The central Cu(II) metal ion of each of these complexes appears to be coordinated to 2–4 dendrimer tertiary amine groups located in the equatorial plane and 2 axial water molecules. Finally, we combine the results of our experiments with literature data to formulate and evaluate a phenomenological model of Cu(II) uptake by G_x-NH₂ PAMAM dendrimers in aqueous solutions. At low metal ion–dendrimer loadings, the model provides a good fit of the measured extent of binding of Cu(II) in aqueous solutions of G₄-NH₂ and G₅-NH₂ PAMAM dendrimers at pH 7.0.

Introduction

Advances in macromolecular chemistry such as the invention of dendritic polymers are providing unprecedented opportunities to develop high-capacity nanoscale chelating agents with well-defined molecular composition, size, and shape.^{1–22} Poly(amidoamine) (PAMAM) den-

drimers (the initial focus of this research) possess functional nitrogen and amide groups arranged in regular “branched upon branched” patterns which are displayed in geometrically progressive numbers as a function of generation level. This high density of nitrogen ligands and the possibility of attaching various functional groups such as carboxyl, hydroxyl, and so forth to PAMAM dendrimers make them particularly attractive as high-capacity chelating agents for metal ions. Several inves-

* Corresponding author. Mail: Materials and Process Simulation Center, Beckman Institute MC 139-74, California Institute of Technology, Pasadena, CA, 91125. Phone: 626 395 2730. Fax: 626 585 0918. E-mail: diallo@wag.caltech.edu and mdiallo@wag.caltech.edu.

† California Institute of Technology.

‡ Howard University.

§ University of Michigan.

|| Pacific Northwest National Laboratory.

⊥ University of Nevada.

(1) Newkome, G. R.; Moorefield, C. N.; Vogtle, F. *Dendritic Molecules: Concepts, Syntheses, Perspectives*; VCH: New York, 1996.

(2) Bosman, A. W.; Janssen, H. M.; Meijer, E. W. *Chem. Rev.* **1999**, *99*, 1665–1668.

(3) Zeng, F.; Zimmerman, S. C. *Chem. Rev.* **1997**, *97*, 1681–1712.

(4) *Dendrimers and Other Dendritic Polymers*; Fréchet, J. M. J., Tomalia, D. A., Eds.; Wiley and Sons: New York, 2001.

(5) Diallo, M. S.; Balogh, L.; Shafagati, A.; Johnson, J. H.; Goddard, W. A., III.; Tomalia, D. *Environ. Sci. Technol.* **1999**, *33*, 820–824.

(6) Zhou, L.; Russell, D. H.; Zhao, M. Q.; Crooks, R. M. *Macromolecules* **2001**, *34*, 3567–3573.

(7) Ottaviani, M. F.; Montali, F.; Turro, N. J.; Tomalia, D. A. *J. Am. Chem. Soc.* **1994**, *116*, 661–671.

(8) Ottaviani, M. F.; Bossman, S.; Turro, N. J.; Tomalia, D. A. *J. Phys. Chem. B.* **1997**, *101*, 158–166.

(9) Ottaviani, M. F.; Montali, F.; Romaneli, M.; Turro, N. J.; Tomalia, D. A. *J. Phys. Chem.* **1996**, *100*, 11033–11042.

(10) Bosman, A. W.; Schemming, A. P. H. J.; Janssen, R. A. J.; Meijer, E. W. *Chem. Ber./Recl.* **1997**, *130*, 725–728.

(11) Vassilev, K.; Ford, W. T. J. *J. Polym. Sci., Part A* **1999**, *37*, 2727–2736.

(12) Ottaviani, M. F.; Favuzza, P.; Bigazzi, M.; Turro, N. J.; Jockusch, S.; Tomalia, D. A. *Langmuir* **2000**, *16*, 7368–7372.

(13) Balogh, L.; Tomalia, D. A. *J. Am. Chem. Soc.* **1998**, *120*, 7355–7356.

(14) Zhao, M. Q.; Sun, L.; Crooks, R. M. *J. Am. Chem. Soc.* **1998**, *120*, 4877–4878.

(15) Zhao, M. Q.; Crooks, R. M. *Chem. Mater.* **1999**, *11*, 3379–3385.

(16) Balogh, L.; Valluzzi, R.; Hagnauer, G. L.; Laverdure, K. S.; Gido, S. P.; Tomalia, D. A. *J. Nanopart. Res.* **1999**, *1*, 353–368.

(17) Cohen, S. M.; Petoud, S.; Raymond, K. N. *Chem.–Eur. J.* **2001**, *7*, 272–279.

(18) Esumi, K.; Suzuki, A.; Yamahira, A.; Toriogoe, K. *Langmuir* **2000**, *16*, 2604–2608.

(19) Balogh, L.; Swanson, D. R.; Tomalia, D. A.; Hagnauer, G. L.; McManus, A. T. *Nano Lett.* **2001**, *1*, 18–21.

(20) Zhao, M.; Crooks, R. M. *Angew. Chem., Int. Ed.* **1999**, *38*, 364–366.

(21) Chechik, V.; Crooks, R. M. *J. Am. Chem. Soc.* **2000**, *122*, 1243–1244.

(22) Crooks, R. M.; Zhao, M.; Sun, L.; Chechik, V.; Yeung, L. K. *Acc. Chem. Res.* **2001**, *34*, 181–190.

tigators have used Cu(II) as a probe to characterize metal ion complexation in aqueous solutions of PAMAM dendrimers. Diallo et al.⁵ have combined ultrafiltration with atomic absorption spectrophotometry to measure the extent of binding (EOB) of Cu(II) ions in aqueous solutions of generations G3–G8 PAMAM dendrimers with ethylenediamine (EDA) core and terminal NH₂ groups. For the G3-NH₂, G4-NH₂, and G5-NH₂ PAMAM dendrimers, they reported maximum EOB of 8 ± 1 , 13 ± 1 , and 29 ± 3 Cu(II) ions per dendrimer molecule at metal ion–dendrimer loadings of 11, 18, and 41 Cu(II) ions per dendrimer molecule, respectively. For the G6-NH₂, G7-NH₂, and G8-NH₂ PAMAM dendrimers, Diallo et al.⁵ found maximum EOB of 46 ± 9 , 83 ± 9 , and 153 ± 20 Cu(II) ions per dendrimer molecule at metal ion–dendrimer loadings of 91, 114, and 306 Cu(II) ions per dendrimer molecule, respectively.

Zhou et al.⁶ have combined matrix-assisted laser desorption (MALDI) time-of-flight (TOF) mass spectrometry (MS) with UV–visible spectroscopy to measure the uptake of Cu(II) by G2, G3, G4, and G6 EDA core PAMAM dendrimers with terminal OH groups in aqueous solutions. While their spectroscopic data indicated maximum binding of 4, 8, 16, and 64 Cu(II) ions per molecule for the G2-OH, G3-OH, G4-OH, and G6-OH PAMAM dendrimers, respectively, the MALDI-TOF mass spectra suggested additional binding [up to 12 Cu(II) ions per molecule] for the G3-OH PAMAM dendrimer as the metal ion–dendrimer loading was increased to 32. Zhou et al.⁶ attributed this additional uptake of Cu(II) to the presence of nonspecific metal ion binding sites for Cu(II) within the dendrimers.

Ottaviani et al.^{7,8} have carried out electron paramagnetic resonance (EPR) studies of the structures of Cu(II)–dendrimer complexes in aqueous solutions of PAMAM dendrimers with COO⁻Na⁺ and NH₂ terminal groups. They fitted computed EPR spectra to the measured spectra of the Cu(II)–dendrimer complexes to estimate their magnetic and mobility parameters. By comparing these estimates with reported literature values, Ottaviani et al.⁷ proposed three types of complexes for the dendrimers with terminal COO⁻Na⁺ groups: (i) a Cu^{II}–N₂O₂ complex involving two terminal COO⁻ groups and two tertiary amine groups for the lower generation dendrimers ($G = 0, 1, \text{ and } 2$) at pH 3.0–10.0, (ii) a Cu^{II}–N₄ complex involving four tertiary amine groups for the higher generation dendrimers ($G = 3, 4, 5, 6, \text{ and } 7$) at higher pH (>5.5), and (iii) a Cu^{II}–O₄ complex involving four oxygens [two from the dendrimer terminal carboxyl groups] for all dendrimers at low pH (<4.5). For the G_x-NH₂ PAMAM dendrimers, Ottaviani et al.⁸ postulated three types of complexes between pH 4 and 5: (i) a Cu(H₂O)₆²⁺ complex, (ii) a Cu^{II}–N₂O₂ complex involving two dendrimer terminal NH₂ groups and two water molecules, and (iii) a Cu^{II}–N₄ complex involving two dendrimer tertiary amine groups and two dendrimer terminal NH₂ groups. At pH ≥ 6.0 , the Cu^{II}–N₄ complex was found to be the only species present.⁷

Despite these advances, the uptake of metal ions such as Cu(II) by dendrimers such as PAMAM is still not well understood. A systematic investigation of the effects of metal ion size/acidity, solution pH, background electrolyte concentration, and metal ion–dendrimer loading on the extent of binding of metal ions to PAMAM dendrimers has yet to be carried out. From a more fundamental point of view, little is known of the effects of dendrimer core chemistry (e.g., hydrophobicity) and terminal group chemistry on the metal ion binding capacity and selectivity of PAMAM dendrimers in aqueous solutions. Not much

is also known of the local structures of Cu(II)–PAMAM dendrimer complexes. Thus, key unanswered questions are whether the uptake of metal ions such as Cu(II) by dendrimers such as PAMAM in dilute aqueous solutions involves several processes including (i) specific binding of metal ions to the dendrimers through coordination with their terminal groups, (ii) specific binding of metal ions to the dendrimers through coordination with their tertiary amine groups, and (iii) nonspecific binding of metal ions with water molecules and/or counterions trapped inside the dendrimers.

A more fundamental question is whether the enhanced binding capacity of PAMAM dendrimers for metal ions such as Cu(II) could be attributed to a *dendritic effect*. To address these questions, we have begun a systematic investigation of metal ion uptake by dendrimers in aqueous solutions. This first paper focuses on the binding of Cu(II) to EDA core PAMAM dendrimers in aqueous solutions. We assess the effects of (i) metal ion–dendrimer loading, (ii) dendrimer generation/terminal group chemistry, and (iii) solution pH on the extent of binding of Cu(II) in aqueous solutions of EDA core PAMAM dendrimers. To gain insight into metal ion coordination with PAMAM dendrimers, we use extended X-ray absorption fine structure (EXAFS) spectroscopy to probe the structures of aqueous complexes of Cu(II) with G1-NH₂ and G5-NH₂ EDA core PAMAM dendrimers. Finally, we combine the results of our experiments with literature data to formulate and evaluate a phenomenological model of Cu(II) uptake by G_x-NH₂ EDA core PAMAM dendrimers in aqueous solutions at neutral pH.

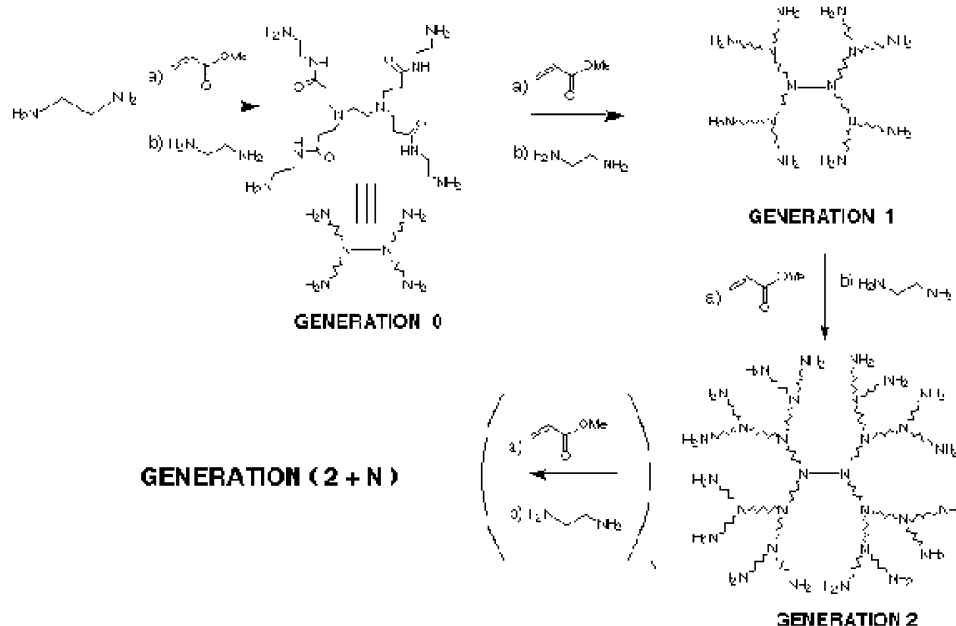
Experimental Section

Dendrimer Synthesis and Characterization. EDA core PAMAM dendrimers (Figure 1) were evaluated in this study. G3-NH₂, G4-NH₂, and G5-NH₂ PAMAM dendrimers with EDA core were purchased from Dendritech (Midland, MI) and used as received. G4 EDA core PAMAM dendrimers with succinic acid (NHCOCH₂CH₂COOH) terminal groups (G4-Sac), glycidylol (NHCH₂CH(OH)CH₂OH) terminal groups (G4-Gly), and acetamide (NHCOCH₃) terminal groups (G4-Ac) were synthesized. All the dendrimers evaluated in this study were characterized by ¹H/¹³C NMR spectroscopy, HPLC, polyacryl amide gel electrophoresis (PAGE), capillary electrophoresis (CE), size exclusion chromatography (SEC), and MALDI-TOF mass spectrometry. Detailed descriptions of the dendrimer synthesis and characterization procedures are given in the Supporting Information.

Acid–Base Titration of Aqueous Solutions of PAMAM Dendrimers. The titration experiments were carried out using a computer-controlled QC-Titrate system from Man-Tech Associates.²³ Prior to each experiment, the instrument was calibrated with certified Fisher buffer solution standards of pH = 4.0, 7.0, and 10.0. Reagent grade HCl and NaOH from Fisher Scientific were used as titrants. In a typical titration experiment, 120 mL of 2.0×10^{-5} M dendrimer solution (in Milli-Q deionized water) was prepared and its pH was adjusted to 3.5 by addition of concentrated HCl. The solution was allowed to equilibrate for 10 min until its pH became stable. A 60 mL aliquot of the dendrimer solution was then transferred into a beaker and titrated with a 0.01 M NaOH solution until its pH reached 11.0. The pK_a's of the dendrimer tertiary amine and terminal groups were taken as the values of the solution pH at the inflection points of the corresponding titration curves.

Measurements of Metal Ion Binding to PAMAM Dendrimers in Aqueous Solutions. Cu(II) was selected as a model cation to probe the binding of metal ions with affinity toward the amine groups of PAMAM dendrimers. Reagent grade Cu(NO₃)₂ from Aldrich was used as a source of Cu(II). For each dendrimer, batch experiments were carried out to determine the extent of

(23) QC-Titrate is a titration/ion analysis system from Man-Tech Associates, <http://www.titrationplus.com/>.



Z- [NH₂; NHCOCH₂CH₂COOH; NHCH₂CH(OH)CH₂OH and NHCOCH₂]

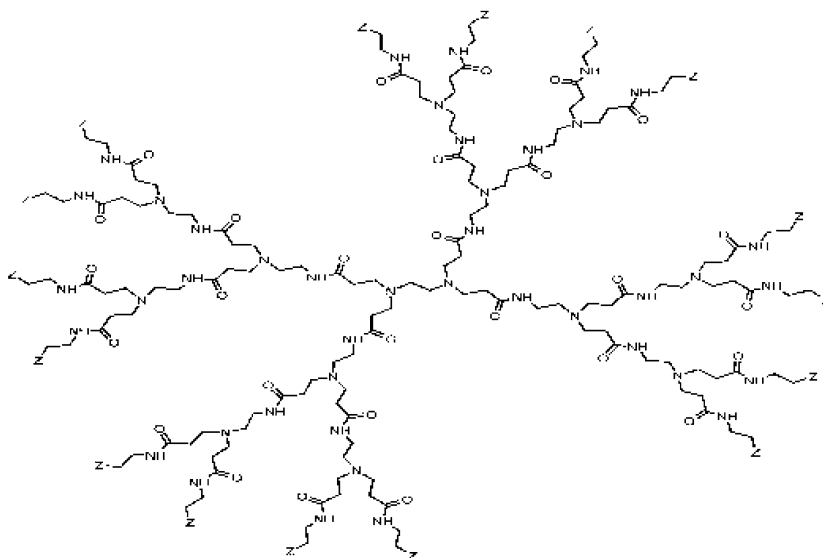


Figure 1. 2-D structures of the dendrimers evaluated in this study as illustrated on EDA core G2 PAMAM dendrimer.

binding of Cu(II) as a function of metal ion–dendrimer loading and solution pH. The binding assay procedure consisted of (i) mixing and equilibrating aqueous solutions of Cu(II) and PAMAM dendrimers at room temperature, (ii) separating the metal ion laden dendrimers from the aqueous solutions by ultrafiltration (UF), and (iii) measuring the pH and copper concentrations of the equilibrated solutions and filtrates.⁵ Preliminary experiments showed that (i) it was possible to control the pH of the solutions within 0.1–0.2 pH unit by addition of concentrated NaOH or HCl and (ii) a mixing time of 30 min was adequate to reach equilibrium. The concentrations of copper in each UF tube (C_{u_0}) and filtrate (C_{u_a}) were measured by atomic absorption spectrophotometry. The concentration of copper bound to a dendrimer (C_{u_b}) (mol/L) was expressed as

$$C_{u_b} = C_{u_0} - C_{u_a} \quad (1)$$

The EOB [i.e., number of moles of bound Cu(II) per mole of dendrimer], the concentration of dendrimer (C_d) in solution (mol/L), and the fractional binding (FB) [i.e., % of Cu(II) bound to the

dendrimers] were expressed as

$$EOB = \frac{C_{u_b}}{C_d} \quad (2)$$

$$C_d = \frac{m_d}{V_s M_{wd}} \quad (3)$$

$$FB = 100 \left(\frac{C_{u_b}}{C_{u_0}} \right) \quad (4)$$

where m_d (g) is the mass of dendrimer in solution, V_s (L) is the solution volume, and M_{wd} (g/mol) is the theoretically estimated molar mass of the corresponding pure and monodisperse dendrimer.

EXAFS Spectroscopic Investigations of Cu(II)–PAMAM Dendrimer Complexes in Aqueous Solutions. EXAFS spectroscopy was used to probe the structures of Cu(II) complexes with G1-NH₂ and G5-NH₂ EDA core PAMAM dendrimers in

aqueous solutions. The copper concentration (0.012 M), the molar ratio of Cu(II) to dendrimer NR₃ groups (1:4), and the solution pH = 7.0 were kept constant for both samples. A 0.012 M Cu(II) solution in Milli-Q deionized water was used as a control. Reagent grade Cu(NO₃)₂ from Aldrich was also used as a source of Cu(II). The Cu K-edge X-ray absorption spectra were collected at the Stanford Synchrotron Radiation Laboratory (SSRL) using wiggler beam line 4-3. The beam energy was 3.0 GeV, and the beam current ranged from 40 to 100 mA. A silicon (220) monochromator was employed to select the incident beam, which was subsequently detuned by 30–50% to remove contributions from higher order harmonics. The beam energy was calibrated using a Cu foil by assigning the first inflection point of the absorption edge to 8980.3 eV. Spectra of aqueous solutions of Cu(NO₃)₂ and Cu(II)–dendrimer aqueous solutions were collected at room temperature over the energy range of 8700–9500 eV in fluorescence mode using a 13-element Ge array detector. Multiple scans were acquired in all experiments to obtain spectra with adequate signal-to-noise ratio.

The spectra were analyzed using the EXAFSPAK software.²⁴ The background was subtracted by fitting a straight line to the pre-edge region. The EXAFS oscillations [$\chi(k)$, where k is the photoelectron wavenumber] were isolated by a third-order spline fit with 3 segments and normalized using a Victoreen polynomial with McMaster coefficients. The normalized EXAFS oscillations were weighted by k^3 to account for the reduction in the amplitude of their oscillations with increasing k . They were then Fourier transformed with an unsmoothed window to isolate different shells and determine their radial distribution functions (RDFs). The identity of the backscattering atoms, the distances between the central absorbing atom and backscattering atoms (R), the coordination numbers (CN) [i.e., the number of neighboring atoms to the central absorbing atom], and the Debye–Waller factors (σ^2) were determined by fitting the EXAFS spectra using phase and amplitude functions calculated by the software Feff 7.02.²⁵ The fitting procedure was carried out in two steps. First, the normalized EXAFS spectra were filtered and fitted using the theoretically calculated phase and amplitude functions. The results of the first fit were employed as starting values for a second fit using the normalized spectra. Because the parameters of the first and second peaks did not significantly change during the second fit, the values of R , CN, and σ^2 for these peaks were fixed to decrease the number of adjustable parameters. The threshold energy, E_0 (i.e., the minimum energy required to eject a photoelectron), was selected as the energy at the top of the absorption peak. A single value of E_0 was used for all shells and allowed to vary during curve fitting. Because of low signal-to-noise ratio, the control Cu(II) solution sample was not included in the EXAFS data analysis.

Results and Discussion

Dendrimer Characterization. The issues of dendrimer purity and monodispersity have received some attention in the literature.^{26–27} Hummelen et al.²⁶ used electrospray ionization (ESI) mass spectrometry to characterize the polydispersity and dendritic purity (defined as the percentage of defect-free dendritic materials) of polypropylene imine (PPI) dendrimers with diamino butane (DAB) core and terminal NH₂ groups. They reported a polydispersity index of 1.002 and a dendritic purity of 23% for the G5-NH₂ DAB core PPI dendrimer. Tolic et al.²⁷ used ESI Fourier transform ion cyclotron resonance (FT-ICR) mass spectrometry to characterize the polydispersity and dendritic purity of G x -NH₂ EDA

Table 1. Selected Properties of the EDA Core PAMAM Dendrimers Evaluated in This Study

dendrimer	theoretical M_w (Da)	measured M_w (Da)	theoretical number of tertiary N groups	theoretical number of terminal groups
G3-NH ₂	6 906	6 910 ^a	30	32
G4-NH ₂	14 215	13 734 ^b	62	64
G4-Gly	20 615	19 365 ^b	62	128
G4-Sac	18 951	18 685 ^b	62	64
G4-Ac	16 903	16 112 ^b	62	64
G5-NH ₂	28 826	23 700 ^b	126	128

^a ESI MS data provided by Dendritech (<http://www.dendritech.com>). ^b MALDI-TOF MS data (this work).

core PAMAM dendrimers. They found that the lower generation dendrimers (G1–G4) had a polydispersity index of 1.0003 and fewer defects (e.g., missing repeat units, intramolecular cyclization and dimer formation) than the higher generation dendrimers (G5–G10). Figures S1, S2, and S3 of the Supporting Information highlight a typical characterization data set for the dendrimers evaluated in this study as illustrated on the G5-NH₂ EDA core PAMAM dendrimer. This compound contains more impurities and defects than any of the dendrimers evaluated in this study. The HPLC data (Figure S2) indicate that the G5-NH₂ PAMAM dendrimer contains relatively small amounts (approximately 0.026 wt %) of unreacted ethylenediamine. The MALDI-TOF mass spectrum (Figure S2) shows that the dendrimer sample also contains defects such as a lower generation EDA core PAMAM dendrimer and a higher molecular weight byproduct. From the SEC data (Figure S3), the weight-average molar mass of the G5-NH₂ EDA core PAMAM dendrimer is estimated to be equal to 26 040 Da. All the remaining dendrimers evaluated in this study exhibit molar mass within 94–100% of the theoretically estimated molar mass of the corresponding pure and monodisperse dendrimers (Table 1).

Protonation of EDA Core PAMAM Dendrimers in Aqueous Solutions. The mechanism of protonation of dendrimers with ionizable groups is the subject of ongoing debate in the literature.^{28–30} Koper and co-workers²⁸ characterized the protonation of G x -NH₂ DAB core PPI dendrimers in aqueous solutions using an integrated experimental and theoretical framework combining potentiometric titrations and ¹⁵N solution NMR with an Ising-like site-binding model of protonation. They concluded that these dendrimers protonate in two consecutive steps with an intermediate plateau at a degree of protonation of 2/3 when they are titrated with concentrated HCl. First, the terminal NH₂ groups of the dendrimers and the tertiary amine groups of their odd shells protonate at pH 10. This is followed by the protonation of the tertiary amine groups from the dendrimer even shells at pH 5. Kabanov et al.³⁰ carried out potentiometric titrations of DAB core PPI dendrimers with terminal NH₂ groups in aqueous solutions. They successfully used the much simpler Henderson–Hasselbach equation (eq 5) to analyze their titration data and estimated the pK_a of the dendrimer NH₂ and tertiary amine groups to be equal to 9.80 and 6.0, respectively.

(24) George, G. N.; Pickering, I. J. *EXAFSPAK: A Suite of Computer Programs for Analysis of X-Ray Absorption Spectra*; Stanford Synchrotron Radiation Laboratory: Stanford, CA, 1995.

(25) Zabinsky, S. I.; Rehr, J. J.; Ankudinov, A.; Albers, R. C.; Eller, M. J. *Phys. Rev. B* **1995**, *52*, 2995–3009.

(26) Hummelen, J. C.; van Dongen, J. L. J.; Meijer, E. W. *Chem.—Eur. J.* **1997**, *3*, 1489–1493.

(27) Tolic, L. P.; Anderson, G. A.; Smith, R. D.; Brothers, H. M.; Splindler, R.; Tomalia, D. *Int. J. Mass. Spectrom. Ion Processes* **1997**, *165/166*, 405–418.

(28) Koper, G. J. M.; van Genderen, M. H. P.; Elissen-Roman, C.; Baars, M. W. P.; Meijer, E. W.; Borkovec, M. *J. Am. Chem. Soc.* **1997**, *119*, 6512–6521.

(29) van Duijvenbode, R. C.; Rajanayagam, A.; Koper, G. J. M.; Baars, M. W. P.; de Waal, B. F. M.; Meijer, E. W.; Borkovec, M. *Macromolecules* **2000**, *33*, 46–52.

(30) Kabanov, V. A.; Zezin, A. B.; Rogacheva, V. B.; Gulyaeva, V. B.; Zansochova, M. F.; Joosten, J. G. H.; Brackman, J. *Macromolecules* **1998**, *31*, 5142–5144.

Table 2. Measured pK_a and Literature Data for the Tertiary Amine and Terminal NH_2 , Gly ($NHCH_2CH(OH)CH_2OH$), Sac ($NHCOCH_2CH_2COOH$), and Acetamide ($NHCOCH_3$) Groups of the EDA Core PAMAM Dendrimers Evaluated in This Study

dendrimers	pK_a of tertiary N groups (this work)	pK_a of terminal groups (this work)	pK_a of tertiary N groups (literature)	pK_a of terminal groups (literature)
G3-NH ₂	6.52	9.90	6.70 ^a –6.30 ^b	9.00 ^a –9.23 ^b
G4-NH ₂	6.85	10.29	6.70 ^a –6.30 ^b	9.00 ^a –9.23 ^b
G4-Gly	7.09	11.0		
G4-Sac	6.75	10.58		
G4-Ac	6.72	NA ^c		
G5-NH ₂	7.16	10.77	6.70 ^b –6.30 ^b	9.00 ^a –9.23 ^b

^a Data taken from Cakara et al. (ref 32). ^b Data taken from Niu et al. (ref 33). ^c Not applicable. The G4-Ac EDA core PAMAM dendrimer has terminal $NHCOCH_3$ groups.

The titration curves of the PAMAM dendrimers evaluated in this work are shown in Figures S4–S9 of the Supporting Information. We fitted each titration curve with a sigmoid function and subsequently used the Mathematica version 4 software³¹ to find the inflection points of each titration curve. The pK_a 's of the dendrimers' tertiary amine and terminal groups were taken as the values of the solution pH at the inflection points of the titration curves. The pK_a 's of the tertiary amine groups of the G3-NH₂, G4-NH₂, and G5-NH₂ PAMAM dendrimers are equal to 6.52, 6.85, and 7.16, respectively (Table 2). They compare favorably with the pK_a of the tertiary amine groups of G_x-NH₂ EDA core PAMAM dendrimers (6.70 and 6.30) reported by Cakara et al.³² and Niu et al.³³ The measured pK_a 's of the terminal NH₂ groups for the G3-NH₂, G4-NH₂ EDA, and G5-NH₂ EDA core PAMAM dendrimers are equal to 9.90, 10.29, and 10.77, respectively (Table 2). However, in this case, these values are higher (by 1–1.5 pK_a units) than the pK_a values of the NH₂ groups of EDA core PAMAM dendrimers (9.0 and 9.23) reported by Cakara et al.³² and Niu et al.³³ Although these investigators have employed theoretically derived protonation models to analyze their titration data, independent experimental measurements and/or atomistic simulations have not validated their models. Thus, we are not sure how significant are the differences between our estimated pK_a and those reported by Cakara et al.³² and Niu et al.³³ Table 2 also shows that the pK_a 's of the tertiary amine groups (6.75, 7.09, and 6.72) of the G4-Gly, G4-Sac, and G4-Ac EDA core PAMAM dendrimers are comparable

(31) *Mathematica*, version 4; Wolfram Research: Champaign, IL, 1999; <http://www.wolfram.com>.

(32) Cakara, D.; Kleiman, J.; Borkovec, M. *Macromolecules* **2003**, *36*, 4201–4207. These authors used a site binding model analogous to the classical Ising model to analyze the measured titration curves of EDA core G_x-NH₂ PAMAM dendrimers in aqueous solutions. The model has six adjustable parameters including three "microconstants" for the dendrimer primary amine groups ($pK_a^{(1)}$), tertiary amine groups ($pK_a^{(III)}$), and innermost tertiary amine groups ($pK_a^{(III)}$) along with three nearest neighbor interaction parameters (ϵ , ϵ' , and ϵ''). These parameters were determined by nonlinear least-squares fitting of the measured titration curves for two low-generation (G0-NH₂ and G1-NH₂) EDA core PAMAM dendrimers. Cakara et al. (ref 32) subsequently used these parameters to investigate the protonation of higher generation EDA core PAMAM dendrimers.

(33) Niu, Y.; Sun, L.; Crooks, R. M. *Macromolecules* **2003**, *36*, 5725–5731. These authors used a multishell structural model and a Frumkin adsorption isotherm to analyze the measured titration curves of EDA core G4-NH₂ and G4-OH PAMAM dendrimers in aqueous solutions. Their analysis yielded two parameters: an intrinsic proton binding constant and "a constant that characterizes the strength of electrostatic interactions among occupied binding sites". Based on the results of their analysis, Niu et al. (ref 33) estimated the pK_a of the tertiary amine groups of G4-NH₂ and G4-OH EDA PAMAM dendrimers to be respectively 6.30. They also reported a pK_a of 9.23 for the primary amine groups of the G4-NH₂ PAMAM dendrimer.

Table 3. Extents of Protonation^a of the Tertiary Amine and Terminal Groups of the EDA Core PAMAM Dendrimers Evaluated in This Study

A. Fraction of Protonated Tertiary Amine Groups				
dendrimers	pH 3	pH 5	pH 7	pH 9
G3-NH ₂	0.99	0.94	0.14	0.001
G4-NH ₂	0.99	0.97	0.26	0.003
G4-Gly	0.99	0.98	0.31	0.004
G4-Sac	0.99	0.96	0.21	0.003
G4-Ac	0.99	0.97	0.23	0.004
G5-NH ₂	0.99	0.99	0.42	0.007
B. Fraction of Protonated Terminal Groups				
dendrimers	pH 3	pH 5	pH 7	pH 9
G3-NH ₂	0.99	0.99	0.99	0.80
G4-NH ₂	0.99	0.99	0.99	0.88
G4-Gly	1.00	1.00	1.00	1.00
G4-Sac	0.99	0.99	0.99	0.91
G4-Ac	NA	NA	NA	NA
G5-NH ₂	0.99	0.99	0.99	0.94

^a Evaluated using eqs 5 and 6. The electrostatic repulsion parameters between (i) two protonated nearest neighbor tertiary amine groups ($\epsilon_{N-N} = 0.15$), (ii) two protonated nearest neighbor primary and tertiary amine groups ($\epsilon_{N-NH_2} = 0.15$), and (iii) two protonated nearest neighbor primary amine groups ($\epsilon_{NH_2-NH_2} = 0.14(G-1)$ where $G \geq 2$ is the dendrimer generation) were taken from Cakara et al. (ref 32). The electrostatic repulsion parameter between two protonated nearest neighbor tertiary amine and succinamic acid groups ($\epsilon_{N-Sac} = 0.5$) of the EDA core G4-Sac PAMAM dendrimer was assumed to be equal to that between a tertiary amine and a carboxyl group (ϵ_{NCOO}) reported by van Duijvenbode et al. (ref 29). Because the terminal glycidol groups of the G4-Gly dendrimer are neutral, the measured pK_a (11.0) of this dendrimer was used in eq 5 to calculate the extent of protonation of its terminal groups.

to those of the G_x-NH₂ PAMAM dendrimers. Since most aliphatic alcohols have pK_a values of > 14 ,³⁴ a pK_a of 11.0 seems reasonable for the terminal glycidol ($NHCH_2CH(OH)CH_2OH$) groups of the G4-Gly PAMAM dendrimer. However, the pK_a (10.58) of the terminal succinamic acid ($NHCOCH_2CH_2COOH$) groups is substantially higher than the pK_a (≈ 4.0) of the carboxyl groups of DAB core PPI dendrimers with lithium carboxylate (COO^-Li^+) terminal groups.²⁹ Although this could be partly attributed to structural differences between the two classes of dendrimers, at the present time, we have no clear explanation for this difference.

Table 3 summarizes the estimated extents of protonation (α) of the tertiary amine and terminal groups of the PAMAM dendrimers evaluated in this study. They were calculated using the Henderson–Hasselbach equation³⁰ with an effective pK_a^i that takes into account electrostatic repulsion between two protonated nearest neighbor sites i and j :^{28–29,32}

$$\log \frac{\alpha}{1-\alpha} = p\tilde{K}_a^i - pH \quad (5)$$

$$p\tilde{K}_a^i = pK_a^i - \sum_j \epsilon_{ij} \quad (6)$$

where pK_a^i is the measured pK_a of dendrimer group i (Table 2) and ϵ_{ij} is the electrostatic repulsion between two protonated nearest neighbor dendrimer groups i and j (Table 3). All the amine groups of the G_x-NH₂ EDA core PAMAM dendrimers become protonated at low pH (≤ 5), whereas at neutral pH (≈ 7.0), only their tertiary amine groups remain unprotonated (Table 3). Note that these results are similar to those reported by Cakara et al.³² and Niu et al.³³ The overall results of the acid–base

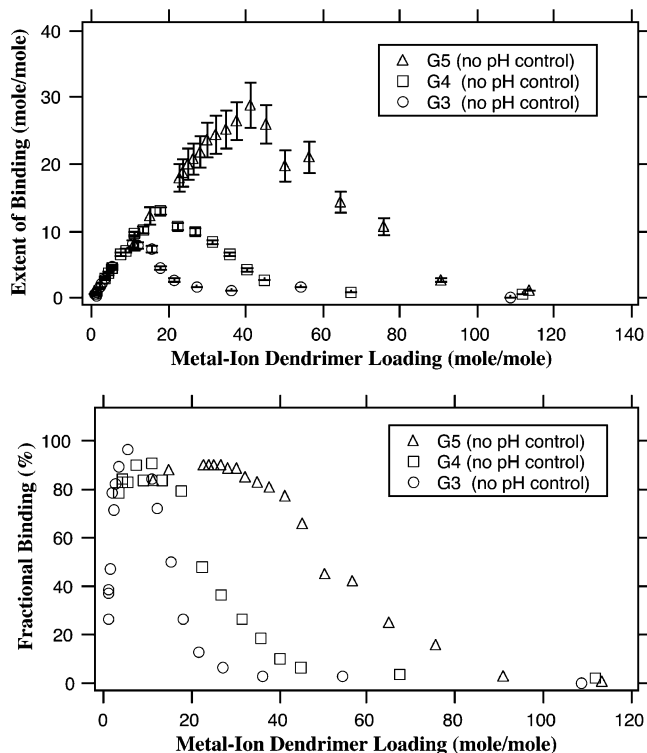


Figure 2. Extent of binding and fractional binding of Cu(II) ions in aqueous solutions of EDA core PAMAM dendrimers as a function of metal ion–dendrimer loading at room temperature and no pH control. Data are taken from Diallo et al. (ref 5).

titration experiments suggest that (i) the tertiary amine and terminal groups of EDA core PAMAM dendrimers protonate independently and (ii) dendrimer generation and terminal group chemistry do not have a significant impact on the extent of protonation of the tertiary amine groups of EDA core PAMAM dendrimers.

Effects of Metal Ion–Dendrimer Loading, Solution pH, Dendrimer Generation and Terminal Group Chemistry on Cu(II) Binding to EDA Core PAMAM Dendrimers. As previously stated, Diallo et al.⁵ and Zhou et al.⁶ have reported measurements of the extent of binding of Cu(II) in aqueous solutions of EDA core PAMAM dendrimers. However, in both of these studies, the pH of the Cu(II)–dendrimer solutions was not kept constant. Figure 2 highlights the effect of metal ion–dendrimer loading on the EOB and FB of Cu(II) in aqueous solutions of $G_x\text{-NH}_2$ EDA core PAMAM dendrimers with no pH control. The data and error bars are taken from Diallo et al.⁵ Both the EOB and FB of Cu(II) go through a maximum as metal ion–dendrimer loading increases. Figures 3 and 4 illustrate the effects of metal ion–dendrimer loading and solution pH on the EOB and FB of Cu(II) in aqueous solutions of the $G_x\text{-NH}_2$ EDA core PAMAM dendrimers. In these experiments, we varied the Cu(II)–dendrimer NH_2 group molar ratio (from 0.02 to 2.0) to prepare solutions with a given metal ion–dendrimer loading. To highlight the reproducibility of the data, we have included three replicate measurements of Cu(II) binding to the $G_4\text{-NH}_2$ and $G_5\text{-NH}_2$ PAMAM dendrimers. At pH 9, the EOB of Cu(II) increases linearly with metal ion–dendrimer loading within the range of tested metal ion–dendrimer loadings (Figure 3). In all cases, 100% of the Cu(II) ions are bound to the dendrimers (Figure 4). We attribute this

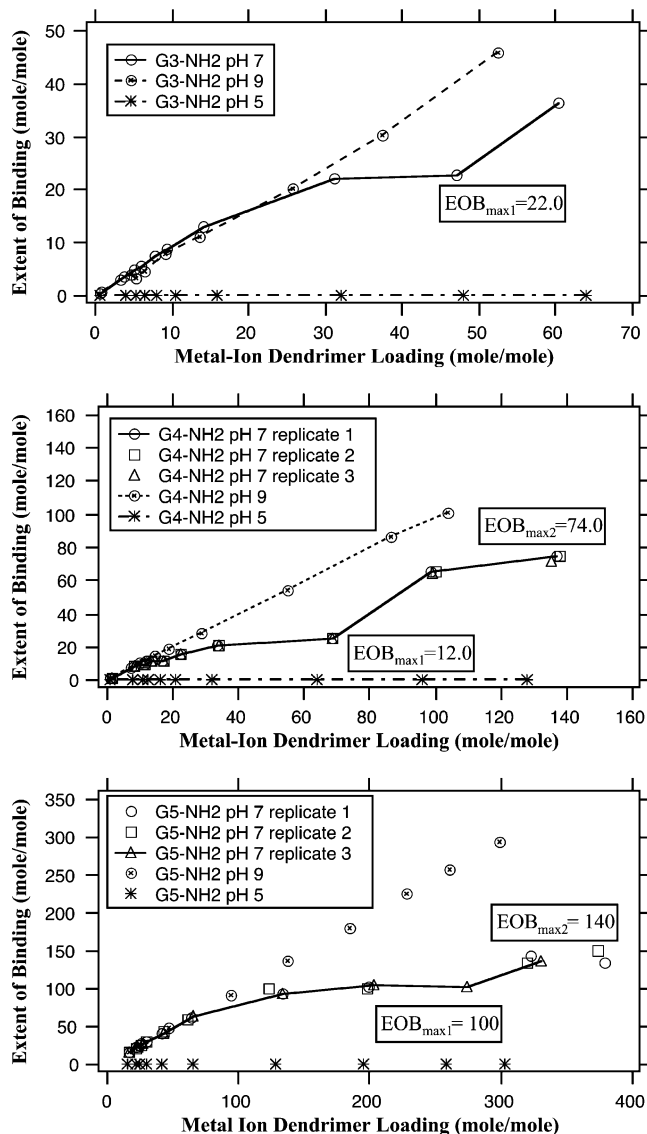


Figure 3. Extent of binding of Cu(II) in aqueous solutions of $G_3\text{-NH}_2$, $G_4\text{-NH}_2$, and $G_5\text{-NH}_2$ EDA core PAMAM dendrimers as a function of solution pH and metal ion–dendrimer loading at room temperature.

behavior to the low extent of protonation of the dendrimer amine groups (Table 3). When these groups become fully protonated at pH = 5.0 (Table 3), no binding of Cu(II) is observed (Figures 3 and 4). A more complex metal ion uptake behavior is observed at pH = 7.0. In this case, the EOB of Cu(II) in aqueous solutions of the $G_x\text{-NH}_2$ PAMAM dendrimers goes through a series of two distinct binding steps as metal ion–dendrimer loading increases (Figure 3). Note that the plateau for the $G_3\text{-NH}_2$ dendrimer [EOB ≈ 22.0 mol of Cu(II) per mole of dendrimer] is comparable in magnitude to the EOB of Cu(II) [≈ 20 mol of Cu(II) per mole of dendrimer] in aqueous solutions of $G_3\text{-OH}$ EDA core PAMAM dendrimer measured by Zhou et al.⁶ The FB of Cu(II) in aqueous solutions of the $G_x\text{-NH}_2$ PAMAM dendrimers also goes through a similar series of distinct binding steps (Figure 4). Because each of these steps involves an initial linear increase in Cu(II) binding followed by a gradual leveling off and a second increase, we attribute this behavior to the presence of sites with different Cu(II) binding affinity and capacity within the dendrimers. Zhou et al.⁶ have also postulated the presence of weak ion-binding sites to account for the additional binding [up to 12 Cu(II) ions per molecule] for $G_3\text{-OH}$

(34) Schwarzenbach, R. P.; Gschwend, P.; Imboden, D. M. *Environmental Organic Chemistry*, 2nd ed.; John Wiley & Sons: Hoboken, NJ, 2003.

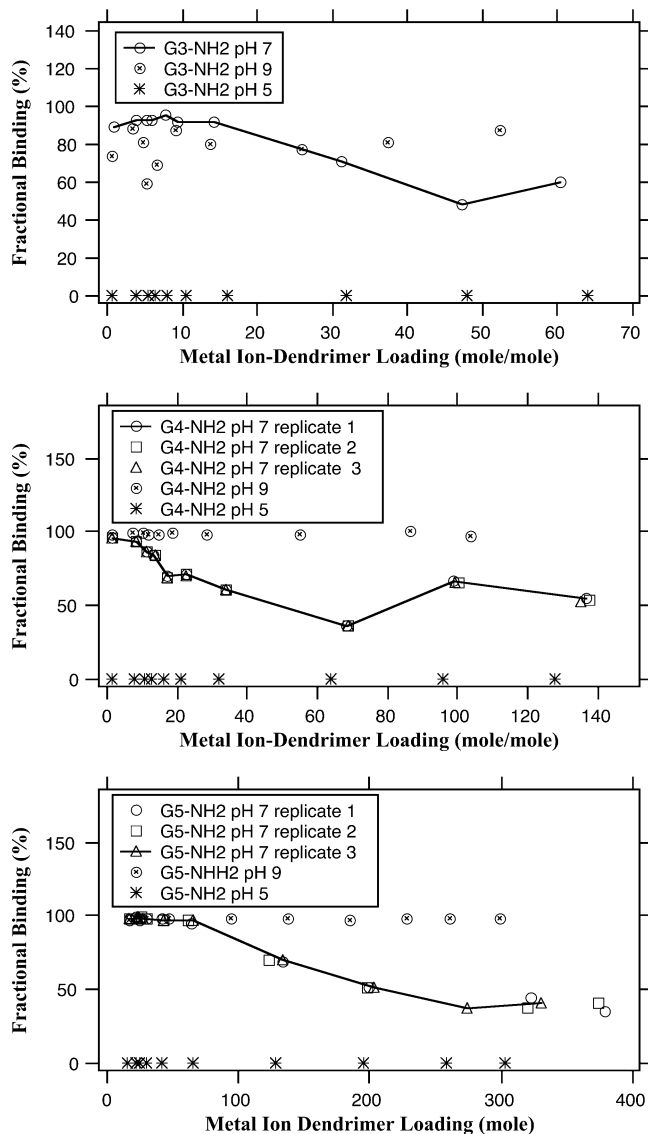


Figure 4. Fractional binding of Cu(II) in aqueous solutions of G3-NH₂, G4-NH₂, and G5-NH₂ EDA core PAMAM dendrimers as a function of solution pH and metal ion–dendrimer loading at room temperature.

PAMAM dendrimer as metal ion–dendrimer loading was increased to 32.

Figures 5 and 6 show the effects of metal ion–dendrimer loading and solution pH on the EOB and FB of Cu(II) in aqueous solutions of the G4-Gly, G4-Sac, and G4-Ac EDA core PAMAM dendrimers. In these experiments, we also varied the Cu(II)–dendrimer terminal group ratios (from 0.02 to 2.0) to prepare solutions with a given metal ion–dendrimer loading. We have also included three replicate measurements of Cu(II) binding to the G4-Sac, G4-Gly, and G4-Ac PAMAM dendrimers at pH 7 to show the reproducibility of the data. Figures 5 and 6 highlight the similarities between the G4-NH₂ and the G4-*x* EDA core PAMAM dendrimers. Here again, the extent of protonation of the dendrimer tertiary amine and terminal groups emerges as a key controlling factor. When these groups are neutral at pH 9 (Table 3), the EOB of Cu(II) also increases linearly with metal ion–dendrimer loading (Figure 5). The FB of Cu(II) is also equal to 100% for all the G4-*x* PAMAM dendrimers (Figure 6). The tertiary amine and terminal groups of the G4-Sac and G4-Ac PAMAM dendrimers become fully protonated at pH 5 (Table 3). Not surprisingly, negligible binding of Cu(II) is

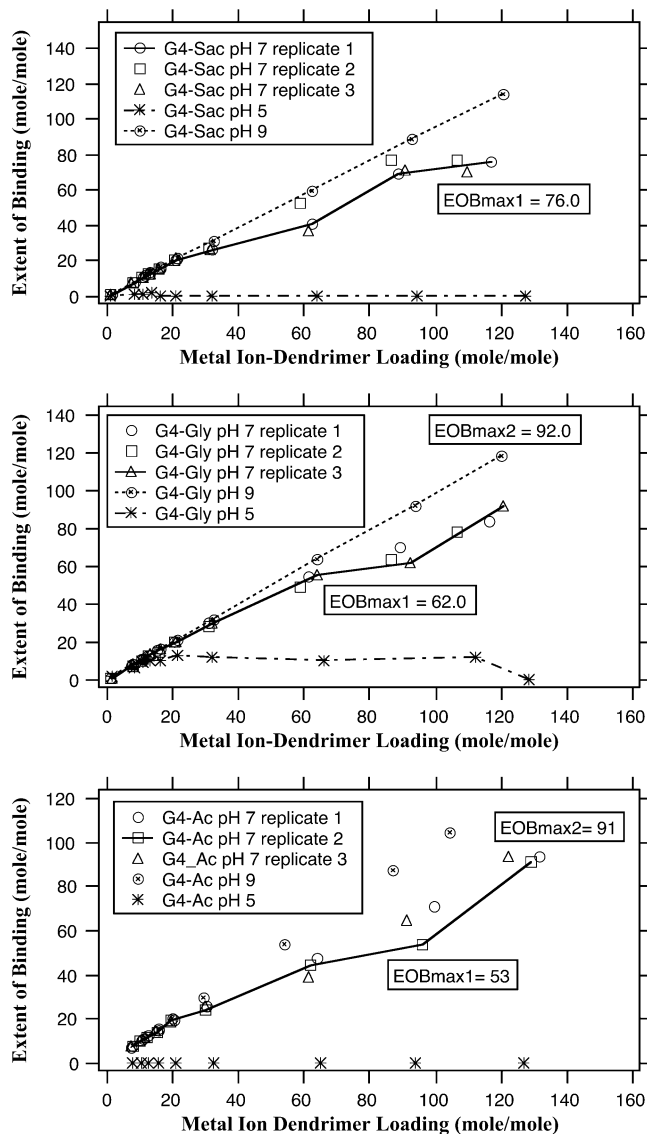


Figure 5. Extent of binding of Cu(II) in aqueous solutions of G4-Sac (NHCOCH₂CH₂COOH), G4-Gly (NHCH₂CH(OH)CH₂-OH), and G4-Ac (NHCOCH₃) EDA core PAMAM dendrimers as a function of solution pH and metal ion–dendrimer loading at room temperature.

observed in these cases (Figures 5 and 6). Conversely, up to 12 Cu(II) ions per mole of dendrimer are bound to the G4-Gly PAMAM dendrimer at pH 5 (Figure 5). The terminal glycidol groups of this dendrimer are not protonated at pH 5.0 (Table 3) and are thus available for metal binding. At pH 7.0, the EOB and FB of Cu(II) ions in aqueous solutions of the G4-*x* functionalized PAMAM dendrimers go through the same series of binding steps as observed for the G_{*x*}-NH₂ PAMAM dendrimers. Here again, we also attribute this behavior to the presence of sites with different Cu(II) binding affinity/capacity within the dendrimers.

Figure 5 provides compelling evidence of the role of the tertiary amine groups in the uptake of Cu(II) by EDA core PAMAM dendrimers in aqueous solutions. The respective roles of the primary/tertiary amine groups in metal ion uptake by PPI and PAMAM dendrimers are still the subject of debate in the literature. Bosman et al.¹⁰ used UV–visible and EPR spectroscopy to characterize the uptake of Cu(II) by DAB core PPI dendrimers in methanol. They reported no Cu(II) binding to the PPI dendrimers with terminal amide groups. For the G_{*x*}-NH₂ PPI den-

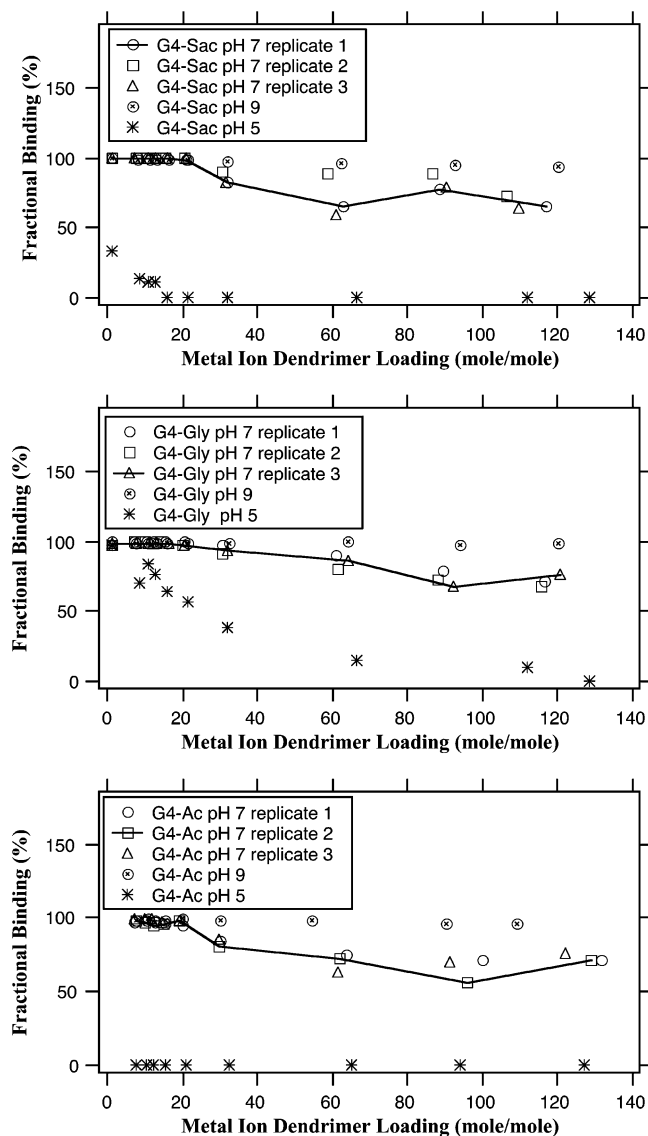


Figure 6. Fractional binding of Cu(II) in aqueous solutions of G4-Sac ($\text{NHCOCH}_2\text{CH}_2\text{COOH}$), G4-Gly ($\text{NHCH}_2\text{CH}(\text{OH})\text{CH}_2\text{OH}$), and G4-Ac (NHCOCH_3) EDA core PAMAM dendrimers as a function of solution pH and metal ion–dendrimer loading at room temperature.

drimers, Bosman et al.¹⁰ found the extent of binding of Cu(II) to be close to $n/2$, where n is the number of dendrimer terminal NH_2 groups. They subsequently took this result as evidence of the absence of interaction of Cu(II) with the dendrimer tertiary amine groups. Conversely, EXAFS spectroscopic investigations of the structures of Cu(II) complexes with $G_x\text{-NH}_2$ PPI dendrimers in methanol³⁵ suggest that each complex consists of a square-based pyramid in which a Cu(II) metal ion is bound to two primary amine groups, one tertiary amine group, and two solvent (i.e., methanol) molecules or NO_3^- counterions. Ottaviani et al.^{7,8} have also provided EPR evidence of Cu(II) coordination with the tertiary amine groups of PAMAM dendrimers in aqueous solutions. Because the G4-Ac EDA core PAMAM dendrimer has terminal acetamide (NHCOCH_3) groups, we anticipate Cu(II) coordination with its tertiary amine groups to be a key mechanism of metal ion uptake. Indeed, when the tertiary amine groups of this dendrimer become fully protonated at pH 5.0 (Table

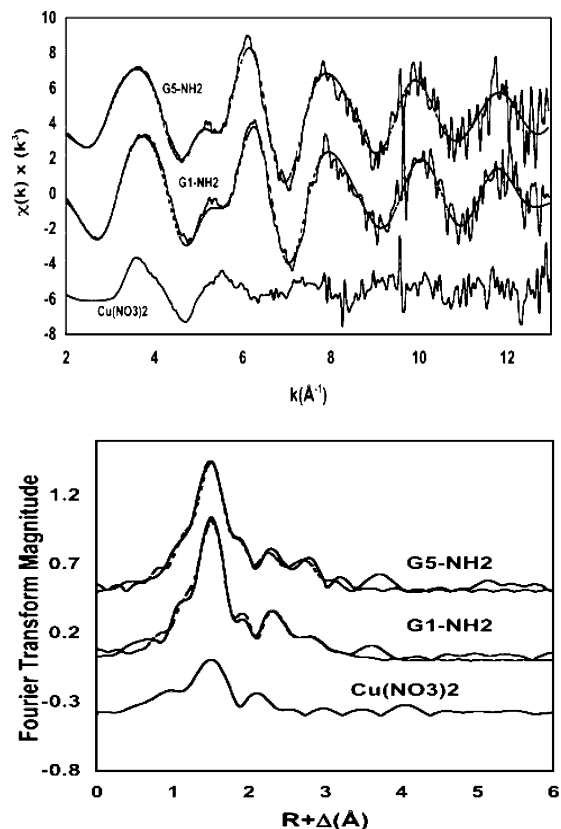


Figure 7. Cu K-edge EXAFS spectra (with Fourier transform) of aqueous solutions of Cu(II) complexes with G1- NH_2 and G5- NH_2 PAMAM EDA core dendrimers and nitrate at room temperature, pH 7, and $\text{Cu}^{\text{II}}\text{-NR}_3$ molar ratio of 1:4. Experimental data (solid line) and nonlinear least-squares fitting (dashed line) are shown.

3), no binding of Cu(II) is observed (Figure 5). Conversely, a significant uptake of Cu(II) is observed when the tertiary amine groups of the G4-Ac PAMAM dendrimer become neutral at pH 7.0 and 9.0. Overall, the metal ion binding measurements in aqueous solutions of the G4-Ac PAMAM dendrimer strongly suggest that metal ion coordination with tertiary amine groups is a significant mechanism of Cu(II) uptake by EDA core PAMAM dendrimers in aqueous solutions.

EXAFS Spectroscopic Investigations of Cu(II)–PAMAM Dendrimer Complexes in Aqueous Solutions. Two key issues guided the design of the EXAFS experiments. Because the protonated NH_2 groups of EDA core dendrimers are not available to bind metal ions at pH 7.0, our first objective was to characterize the coordination of Cu(II) with their tertiary amine groups. A second objective was to gain insight into a potential *dendritic effect* by comparing the structures of Cu(II) complexes with those of an earlier generation dendrimer (G1- NH_2) and a later generation dendrimer (G5- NH_2). Figure 7 shows the k^3 -weighted EXAFS oscillations [$\chi(k)$] of aqueous solutions of Cu(II) with NO_3^- and G1- NH_2 /G5- NH_2 EDA core PAMAM dendrimers [pH 7 and $\text{Cu}^{\text{II}}\text{-NR}_3$ molar ratio of 1:4]. The Fourier transforms (FTs) of the EXAFS spectra are given also in Figure 7. The measured EOB of Cu(II) in aqueous solutions of the G5- NH_2 PAMAM dendrimer is ≈ 31 mol of metal ions per mole of dendrimer. In Figure 7, the solid and dashed lines represent experimental and calculated spectra, respectively. The FTs of the EXAFS spectra are qualitatively similar to those of aqua complexes of Cu(II) with ligands containing nitrogen donors such as EDA and cyclam.³⁶

(35) Floriano, P. N.; Noble, C. O., IV; Schoonmaker, J. M.; Pollakof, E. D.; McCarley, R. L. *J. Am. Chem. Soc.* **2001**, *125*, 10545–10553.

Table 4. Estimated Coordination Number (CN), Bond Distances (R), and Debye–Waller Factors (σ^2) by Nonlinear Least-Squares Fitting^a of the Normalized EXAFS Spectra

dendrimers	shells	CN ^b	R (Å) ^c	σ^2 (Å ²)	ΔE_0	F^d
G1-NH ₂	Cu–N	4.15	2.00	0.00490	–2.63	14
	Cu–O	2.07	2.32	0.0096		
	Cu–C	4.10	2.98	0.0054		
G5-NH ₂	Cu–Cu	1.90	3.04	0.0152	–7.31	18
	Cu–N	4.32	2.00	0.0050		
	Cu–O	1.98	2.39	0.0106		
	Cu–C	3.55	3.13	0.0044		
	Cu–Cu	3.19	3.02	0.0150		

^a The amplitude reduction factor (S_0^2) was set equal to 0.9 during the fitting process. ^b The acceptable error for CN is 20%. ^c The acceptable errors for R are ± 0.02 Å for the first/second shells and ± 0.04 Å for all other shells. ^d The goodness of fit value (the F factor) for the fit residuals was expressed as

$$F = 100 \left(\frac{\sum_{i=1}^N (\text{Data}_i - \text{Model})^2}{\sum_{i=1}^N (\text{Data}_i)^2} \right)$$

They are also similar to FTs of the EXAFS spectra of Cu(II) complexes with G x -NH₂ DAB core PPI dendrimers in methanol.³⁵

Quantitative analysis of the EXAFS spectra combined with literature data^{35–40} enable us to resolve the structures of the Cu(II)–dendrimer complexes. Table 4 lists the estimated bond distances (R) and coordination number (CN) by nonlinear least-squares fitting of the EXAFS spectra using EXAFSPACK²⁴ and Feff 7.02²⁵ calculated phase and amplitude functions. Because oxygen and nitrogen have similar atomic size and electronic configurations, it is difficult to differentiate between copper–nitrogen and copper–oxygen complexes based solely on their EXAFS spectra. The accuracies of the estimated bond distances (R) are approximately equal to ± 0.02 Å for the first and second shells (Table 4). Thus, the estimated bond distances in the first shell (2.0 Å) of the Cu(II)–dendrimer complexes (Table 4) are higher than those of copper–oxygen complexes (1.93–1.96 Å) reported in the literature.^{35–40} Accordingly, we have assigned four nitrogen ligands to the first coordination shell of the Cu(II)–dendrimer complexes. The Cu–N distance of 2.0 Å suggests that the nitrogen ligands are located in the equatorial plane.^{35–40} The values of the Cu–O bond distances (2.32 and 2.39 Å) and Cu–O coordination numbers of 2 point to the formation of octahedral Cu^{II}–N₄O₂ complexes for both PAMAM dendrimers.^{35–40} Since the nitrogen ligands of the Cu(II)–dendrimer complexes could be associated with either the dendrimer tertiary amines or NO₃[–] ions, it is not possible to fully resolve structures of the Cu(II)–dendrimer complexes based on the quantitative analysis of the EXAFS spectra. Thus, we are proposing two mechanisms of Cu(II) coordination with the tertiary amine groups of EDA core PAMAM dendrimers in aqueous solution. The first mechanism (Model1)

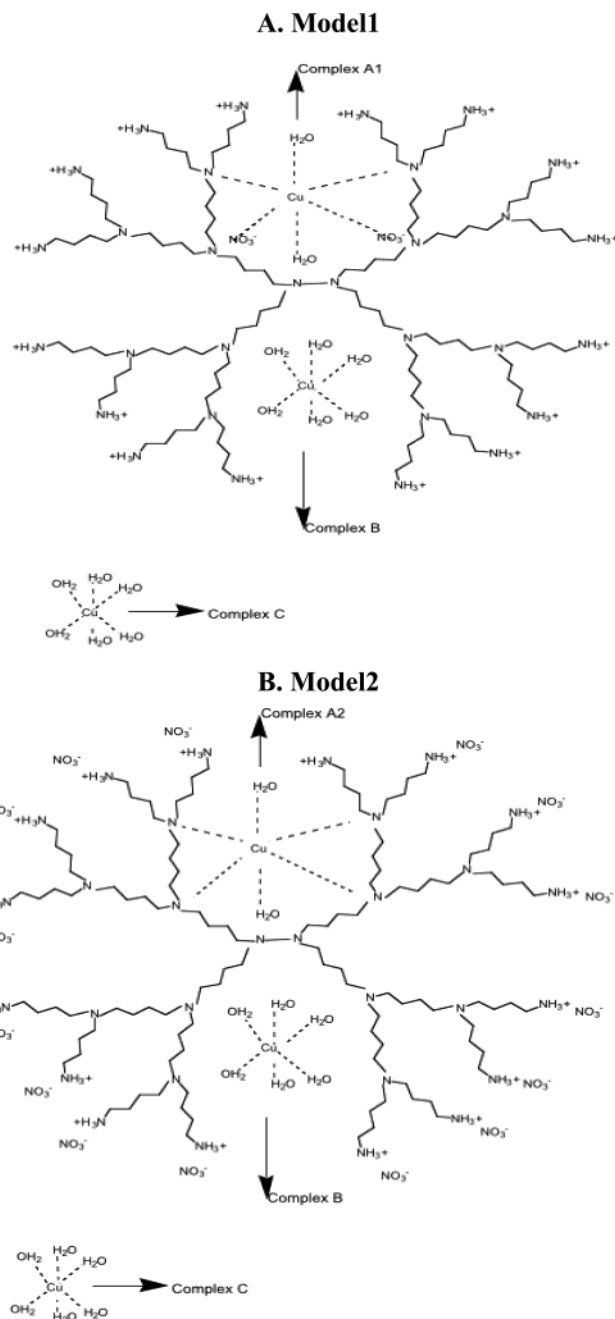


Figure 8. Postulated mechanisms of Cu(II) uptake by G x -NH₂ PAMAM dendrimers in aqueous solutions containing NO₃[–] counterions at room temperature and neutral pH (6 < pH < 9.0).

is illustrated by complex A1 of Figure 8. Here we hypothesize that a Cu(II) metal ion is coordinated with two dendrimer tertiary amine groups and two NO₃[–] counterions. The second mechanism (Model2) is illustrated by complex A2 of Figure 8. In this case, we postulate that a Cu(II) metal ion is coordinated with four dendrimer tertiary amine groups. Although Ottaviani et al.⁶ have provided EPR evidence of Cu^{II}–N₄ complexes involving four tertiary dendrimer amine groups in aqueous solutions of G x -COO[–]Na⁺ PAMAM dendrimers ($x = 3, 4, 5, 6,$ and 7) at higher pH (> 5.5), their coordination models have not been validated by atomistic simulations. Our EXAFS-derived models of Cu(II) coordination with G x -NH₂ PAMAM (Figure 8) have also not been validated by atomistic simulations. Consequently, we have not ruled out other mechanisms of Cu(II) coordination with G x -NH₂ EDA core PAMAM dendrimers in aqueous solutions.

(36) Choy, J.-H.; Kim, D.-K.; Choi, S.-N.; Kim, Y.-J. *Inorg. Chem.* **1997**, *36*, 189–195.

(37) D'Angelo, P.; Bottari, E.; Festa, M. R.; Nolting, H. F.; Pavel, N. V. *J. Phys. Chem. B* **1998**, *102*, 3114–3122.

(38) D'Angelo, P.; Bottari, E.; Festa, M. R.; Nolting, H. F.; Pavel, N. V. *J. Chem Phys.* **1997**, *107*, 2807–2812.

(39) Carrado, K. A.; Wasserman, S. R. *J. Am. Chem. Soc.* **1993**, *115*, 3394–3395.

(40) Person, I.; Person, P.; Sandstrom, M.; Ulstrom, A.-S. *J. Chem. Soc., Dalton Trans.* **2002**, 1256–1265.

Table 4 also shows that 3–4 carbons are coordinated to each Cu(II) ion at an average distance of 3.0 Å. The Cu–Cu coordination number for the G1-NH₂ dendrimer is equal to 1.90 with an average Cu–Cu distance of 3.0 Å. These estimates are also consistent with literature values.³⁵ The value of the Cu–Cu coordination number increases from 1.90 to 3.2 while the Cu–Cu distance remains constant at 3.0 Å for the G5-NH₂ PAMAM dendrimer (Table 4). *We speculate that the substantial increase (≈68%) in the Cu–Cu coordination for the G5-NH₂ PAMAM dendrimer is consistent with a dendritic effect in metal chelation.* A widely held viewpoint in the literature is that a gradual transition in overall shape, from a more extended conformation for earlier generation dendrimers to a more compact/globular shape for later generation dendrimers, causes a significant change in their bulk and solution properties.² One documented signature of this *dendritic effect* is the significant difference between the intrinsic viscosity of a dendrimer and that of a linear polymer of similar molar mass.² Because of their globular shape and the flexibility of their poly(amidoamine) chains, dendrimers such as G5-NH₂ EDA PAMAM can be described as hybrids between linear polymers and soft colloids.^{41–42} Thus, we anticipate the “soft colloid” nature of PAMAM dendrimers [along with their high density of amine groups] to result in a favorable nanoenvironment for the partitioning of metal ions [e.g., Cu(II)], counterions (e.g., NO₃[−]), and solvent molecules (e.g., water). Conversely, the “polymer” character of these dendrimers is expected to endow their poly(amidoamine) chains with the flexibility to coordinate with metal ions located inside the dendrimers or on their external layers. We believe that this dual polymer–colloid character of dendrimers would be at the heart of any *dendritic effect* in metal ion chelation. Additional experiments and molecular dynamics (MD) simulations are underway to test this hypothesis.

Phenomenological Model of Cu(II) Uptake by G_x-NH₂ PAMAM Dendrimers in Aqueous Solutions at Neutral pH. The overall results of the proton and metal ion binding measurements suggest that the uptake of Cu(II) by EDA core PAMAM dendrimers involves both the dendrimer tertiary amine and terminal groups. Figure 3 shows that the EOB of Cu(II) in aqueous solutions of G4-NH₂ and G5-NH₂ PAMAM dendrimers goes through a series of two distinct binding steps at pH 7. Analysis of the EXAFS spectra of the Cu(II) complex with the G5-NH₂ PAMAM dendrimer (Table 4) suggests that the first binding step (which occurs at a Cu^{II}–NR₃ ratio of <1.0) involves the formation of octahedral Cu^{II}–N₄O₂ complexes (see complexes A1 and A2 of Figure 8). We also hypothesize that the second binding step at pH 7.0 involves the formation of octahedral Cu(II) complexes with water molecules trapped inside the PAMAM dendrimers (see complex B of Figure 8). This hypothesis is based on two key observations. First, the protonated terminal NH₂ groups of EDA core PAMAM dendrimers are not able to coordinate with metal ions at pH 7.0. Second, G_x-NH₂ EDA PAMAM dendrimer cores can trap a significant amount of water as shown by recent MD simulations with explicit water molecules.^{43,44} Thus, we anticipate that water molecules trapped inside the EDA core PAMAM dendrimers would also coordinate with Cu(II) ions that are not specifically bound to the dendrimer tertiary amine

groups. Indeed, Ottaviani et al.⁷ have estimated that 20% of Cu(H₂O)₆²⁺ complexes reside in the water pools trapped inside earlier generation G_x-NH₂ PAMAM dendrimers.

Figure 8 provides a conceptual framework for the formulation of a two-site model of Cu(II) uptake by G_x-NH₂ PAMAM dendrimers at neutral pH. Consistent with Tanford's theory of solute binding to macromolecules with noninteracting sites of different intrinsic affinities,⁴⁵ we express the extent of binding of Cu(II) [EOB_{Cu(II)}^d in mole of Cu(II) per mole of dendrimer] in aqueous solutions of EDA core G_x-NH₂ PAMAM at neutral pH as the sum of two terms:

$$\text{EOB}_{\text{Cu(II)}}^{\text{d}} = \text{EOB}_{\text{Cu(II)-N}}^{\text{d}} + \text{EOB}_{\text{Cu(II)-H}_2\text{O}}^{\text{d}} \quad (7)$$

$$\text{EOB}_{\text{Cu(II)-N}}^{\text{d}} = \text{EOB}_{\text{Cu(II)-N}}^{\text{dmax}} \frac{k_{\text{Cu(II)-N}}^{\text{d}} (N_{\text{Cu0}}/N_{\text{d}})}{1.0 + k_{\text{Cu(II)-N}}^{\text{d}} (N_{\text{Cu0}}/N_{\text{d}})} \quad (8)$$

$$\text{EOB}_{\text{Cu(II)-H}_2\text{O}}^{\text{d}} = \text{EOB}_{\text{Cu(II)-H}_2\text{O}}^{\text{dmax}} \frac{k_{\text{Cu(II)-H}_2\text{O}}^{\text{d}} (N_{\text{Cu0}}/N_{\text{d}})}{1.0 + k_{\text{Cu(II)-H}_2\text{O}}^{\text{d}} (N_{\text{Cu0}}/N_{\text{d}})} \quad (9)$$

where $N_{\text{Cu0}}/N_{\text{d}}$ is the metal ion–dendrimer loading [mole of Cu(II) per mole of dendrimer], $\text{EOB}_{\text{Cu(II)-N}}^{\text{dmax}}$ is the amount of Cu(II) specifically bound to the dendrimer tertiary amine groups, and $\text{EOB}_{\text{Cu(II)-H}_2\text{O}}^{\text{dmax}}$ is the amount of Cu(II) bound to water molecules trapped inside the PAMAM dendrimers. The coefficients $k_{\text{Cu(II)-N}}^{\text{d}}$ and $k_{\text{Cu(II)-H}_2\text{O}}^{\text{d}}$ are the corresponding intrinsic association constants.⁴⁵ Consistent with the hypothesized mechanisms of Cu(II) uptake by G_x-NH₂ PAMAM dendrimers (Figure 8), $\text{EOB}_{\text{Cu(II)-N}}^{\text{dmax}}$ and $\text{EOB}_{\text{Cu(II)-H}_2\text{O}}^{\text{dmax}}$ are given by

$$\text{EOB}_{\text{Cu(II)-N}}^{\text{dmax}} = \frac{N_{\text{N}}^{\text{d}}}{\text{CN}_{\text{Cu(II)-N}}^{\text{d}}} \quad (10)$$

$$\text{EOB}_{\text{Cu(II)-H}_2\text{O}}^{\text{dmax}} = \frac{N_{\text{H}_2\text{O-d}} - 2\text{EOB}_{\text{Cu(II)-N}}^{\text{dmax}}}{\text{CN}_{\text{Cu(II)-H}_2\text{O}}^{\text{d}}} \quad (11)$$

where N_{N}^{d} is the number of dendrimer tertiary amine groups, $N_{\text{H}_2\text{O-d}}$ is the number of water molecules bound to the dendrimers, $\text{CN}_{\text{Cu(II)-N}}^{\text{d}}$ is the coordination number of Cu(II) with the dendrimer tertiary amine groups (see complexes A1 and A2 of Figure 8), and $\text{CN}_{\text{Cu(II)-H}_2\text{O}}^{\text{d}}$ is the coordination number of Cu(II) with water molecules trapped inside the dendrimers (see complex B of Figure 9). Equations 7–11 provide a quantitative framework for estimating the extent of binding of Cu(II) in aqueous solutions (at neutral pH) of G_x-NH₂ PAMAM dendrimers as a function of metal ion–dendrimer loading ($N_{\text{Cu0}}/N_{\text{d}}$), dendrimer structural and physicochemical properties (N_{N}^{d} and $N_{\text{H}_2\text{O-d}}$), and metal ion–dendrimer affinity ($k_{\text{Cu(II)-N}}^{\text{d}}$, $k_{\text{Cu(II)-H}_2\text{O}}^{\text{d}}$, $\text{CN}_{\text{Cu(II)-N}}^{\text{d}}$, and $\text{CN}_{\text{Cu(II)-H}_2\text{O}}^{\text{d}}$).

Figure 9 highlights the results of a preliminary evaluation of the two-site model of Cu(II) uptake in aqueous solutions of EDA core G4-NH₂ and G5-NH₂ PAMAM dendrimers at neutral pH. In these calculations, the number of dendrimer tertiary amine groups (N_{N}^{d}) was

(41) Harreis, H. M.; Likos, C. N.; Ballauf, M. *J. Chem. Phys.* **2003**, *118*, 1979–1988.

(42) Rathgeber, S.; Monkenbusch, M.; Kreitschmann, M.; Urban, V.; Brulet, E. *J. Chem. Phys.* **2002**, *117*, 4047–4062.

(43) Lee, I.; Athey, B. D.; Wetzel, A. W.; Meixner, W.; Baker, J. R. *Macromolecules* **2002**, *35*, 4510–4520.

(44) Maiti, P. K.; Cagin, T.; Goddard, W. A., III *Macromolecules*, submitted.

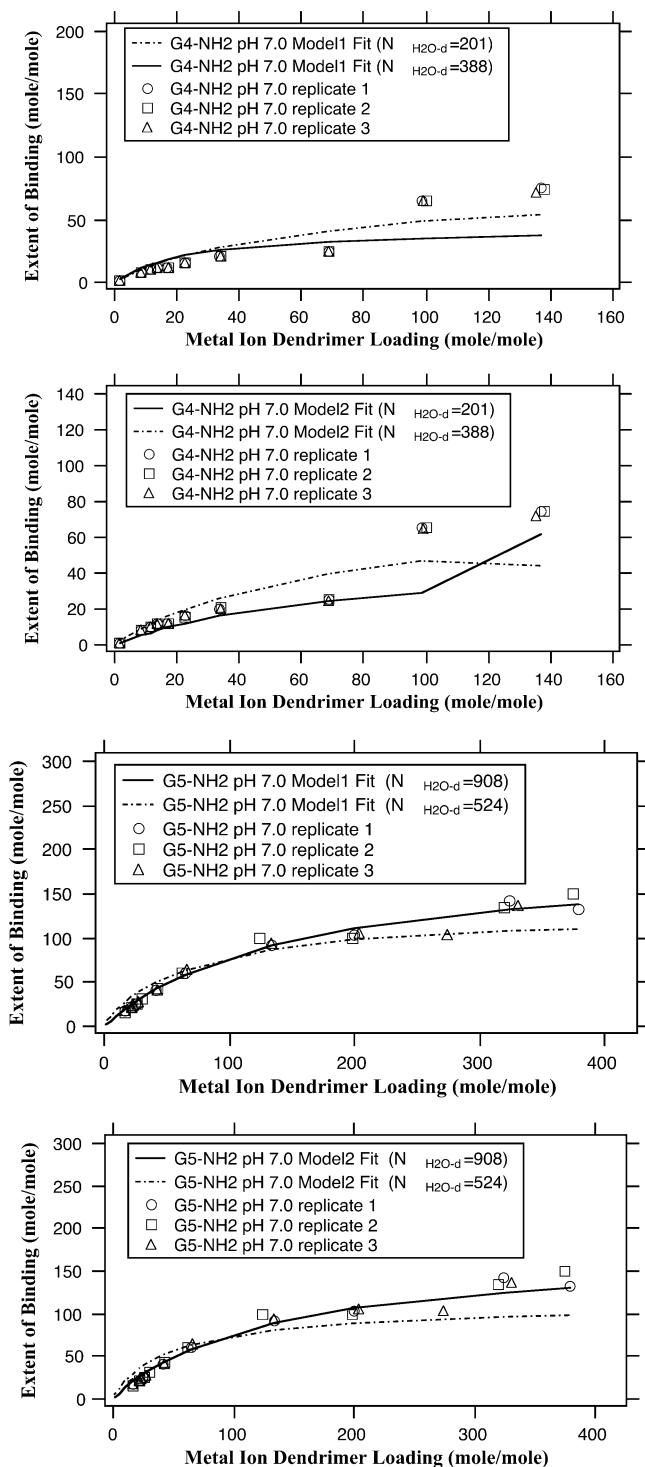


Figure 9. Two-site model of Cu(II) uptake by G4-NH₂ and G5-NH₂ EDA core PAMAM dendrimers in aqueous solutions: calculated versus measured extent of binding at room temperature and pH 7.0.

assumed to be equal to those of the corresponding pure and monodisperse dendrimers (Table 1). The coordination numbers of Cu(II) with the dendrimer tertiary amine groups and trapped water molecules ($CN_{Cu(II)-N}^d$ and $CN_{Cu(II)-H_2O}^d$) are taken from Figure 8. The number of water molecules trapped inside the dendrimers (N_{H_2O-d}) was provided by Maiti et al.⁴⁴ They have successfully used MD simulations with explicit solvent to estimate minimum and maximum values for the extent of binding of water molecules to G_x-NH₂ EDA core PAMAM dendrimers at

high, neutral, and low pH. The association constants $K_{Cu(II)-N}^d$ and $K_{Cu(II)-H_2O}^d$ [expressed in mole of dendrimer per mole of Cu(II)] are the only parameters that were determined by nonlinear least-squares fitting of the experimental data. The parameters used to evaluate the models are given in Table 5. As shown in Figure 9, Model2 provides a better fit of the experimental data than Model1. At low metal ion–dendrimer loadings, both Model1 and Model2 provide good fits of the measured EOB of Cu(II) for the dendrimers (Figure 9). Note that for the G4-NH₂ PAMAM dendrimer, Model2 also reproduces the increase in the EOB of Cu(II) observed at higher metal ion–dendrimer loadings following the first plateau (Figure 3). However, Model1 fails to capture this trend. Additional experiments and MD simulations are underway to further assess the validity of the two-site model of metal ion uptake by G_x-NH₂ PAMAM dendrimers in aqueous solutions at neutral pH.

Summary and Conclusions

This paper describes an investigation of the uptake of Cu(II) by EDA core PAMAM dendrimers in aqueous

(45) Tanford, C. *Physical Chemistry of Macromolecules*; John Wiley & Sons: New York, 1961. Conventional models of complexation have typically described metal ion chelation in aqueous solutions as a set of successive reactions between a central metal ion M and a ligand L (refs 46–48):



The *i*th stepwise stability constant (K_i) and overall stability constant (β_i) are readily expressed in terms of the bound metal ion concentrations ($[ML_i]$ and $[ML_{(i-1)}]$), free metal ion concentration ($[M]$), and free ligand concentration ($[L]$) as

$$K_i = \frac{[ML_i]}{[ML_{(i-1)}][L]} \quad (2)$$

$$\beta_i = \frac{[ML_i]}{[M][L]^i} \quad (3)$$

The stability constants of a given metal ion can be determined by fitting experimental data to the corresponding chemical equilibrium and mass balance equations. Although this approach works well for a traditional chelating agent with a limited number of Lewis base donors (e.g., a polydentate ligand or a macrocycle), it is cumbersome and not feasible in many cases for macroligands (e.g., proteins and dendrimers) with a large number of binding sites. In the early 1960s, Tanford (ref 45) formulated a theory of solute binding to macromolecules. This theory describes the binding of small molecules or ions S to a macromolecule P by *n* association constants (k_1, k_2, \dots, k_n):

$$k_1 = \frac{[PS]}{[P][S]}, \quad k_2 = \frac{[PS_2]}{[PS][S]}, \quad \dots, \quad k_n = \frac{[PS_n]}{[PS_{n-1}][S]} \quad (4)$$

where $[PS], [PS_2], \dots, [PS_n]$ are the concentrations of bound solutes, $[P]$ is the free macromolecule concentration, $[S]$ is the free solute concentration, and *n* is the total number of binding sites on the macromolecule. The bound solute concentrations ($[PS], [PS_2], \dots, [PS_n]$) are usually very difficult to measure. However, in most cases, it is possible to measure the extent of binding $\bar{\nu}$ defined as the average number of solutes S associated with each macromolecule P. $\bar{\nu}$ is readily expressed as (ref 45)

$$\bar{\nu} = \frac{k_1[S] + 2k_1k_2[S]^2 + \dots + nk_1k_2\dots k_n[S]^n}{1 + k_1[S] + k_1k_2[S]^2 + \dots + k_1k_2\dots k_n[S]^n} \quad (5)$$

For a macromolecule with n_1, n_2, \dots, n_i noninteracting binding sites of different intrinsic association constants ($k_{int}^{(1)}, k_{int}^{(2)}, \dots, k_{int}^{(i)}$), eq 5 becomes

$$\bar{\nu} = \frac{n_1 k_{int}^{(1)} [S] + n_2 k_{int}^{(2)} [S] + \dots + n_i k_{int}^{(i)} [S]}{1 + k_{int}^{(1)} [S] + k_{int}^{(2)} [S] + \dots + k_{int}^{(i)} [S]} \quad (6)$$

Equation 6 provided the conceptual framework that we used to formulate our two-site model of Cu(II) uptake by G_x-NH₂ PAMAM dendrimers in aqueous solutions.

(46) Hancock, R. D.; Martell, A. E. *Metal Ion Complexes in Aqueous Solutions*; Plenum Press: New York, 1966.

(47) Burgess, J. *Ions in Solution: Basic Principles of Chemical Interactions*; 2nd ed.; Horwood: West Sussex, U.K., 1999.

(48) Stumm, W.; Morgan, J. J. *Aquatic Chemistry. Chemical Equilibria and Rates in Natural Waters*; 3rd ed.; John Wiley & Sons: New York, 1996.

Table 5. Model Parameters Used To Estimate the Extent of Binding of Cu(II) in Aqueous Solutions of G4-NH₂ and G5-NH₂ EDA Core PAMAM Dendrimers at Room Temperature and pH 7.0

Model1						
dendrimers	N_N^d ^a	N_{H_2O-d} ^b	$CN_{Cu(II)-N}^d$ ^c	$CN_{Cu(II)-H_2O}^d$ ^c	$K_{Cu(II)-N}^d$ ^d	$K_{Cu(II)-H_2O}^d$ ^d
G4-NH ₂	62	201	2	6	0.029 70	0.030 92
G4-NH ₂	62	388	2	6	0.014 67	0.013 54
G5-NH ₂	126	524	2	6	0.014 94	0.015 02
G5-NH ₂	126	908	2	6	0.005 28	0.007 45
Model2						
dendrimers	N_N^d ^a	N_{H_2O-d} ^b	$CN_{Cu(II)-N}^d$ ^c	$CN_{Cu(II)-H_2O}^d$ ^c	$K_{Cu(II)-N}^d$ ^d	$K_{Cu(II)-H_2O}^d$ ^d
G4-NH ₂	62	201	4	6	0.043 81	0.042 82
G4-NH ₂	62	388	4	6	0.017 62	0.016 62
G5-NH ₂	126	524	4	6	0.021 19	0.020 58
G5-NH ₂	126	908	4	6	0.009 29	0.007 832

^a N_N^d is the number of dendrimer tertiary amine groups, assumed to be equal to those of the corresponding pure and monodisperse dendrimers (Table 1). ^b N_{H_2O-d} is the number of water molecules bound to the PAMAM dendrimers. Estimates of the minimum/maximum values for N_{H_2O-d} were provided by Maiti et al. (ref 44). ^c Determined by fitting the calculated extent of binding (eqs 7–11) to the measured extents of binding (Figure 3).

solutions. We combined bench scale measurements of proton and metal ion binding to assess the effects of (i) metal ion–dendrimer loading, (ii) dendrimer generation/terminal group chemistry, and (iii) solution pH on the extent of binding of Cu(II) in aqueous solutions of PAMAM dendrimers. G3-NH₂, G4-NH₂, and G5-NH₂ EDA core PAMAM dendrimers and G4 EDA core PAMAM dendrimers with succinamic acid, glycidylol, and acetamide terminal groups were evaluated in this study. The overall results of the proton and metal ion binding measurements suggest that the uptake of Cu(II) by EDA core PAMAM dendrimers in aqueous solutions involves both the dendrimer tertiary amine and terminal groups. However, the extents of protonation of these groups control the ability of the dendrimers to bind Cu(II). When these groups are neutral at pH 9, the EOB of Cu(II) increases linearly with metal ion–dendrimer loading within the ranges of the tested metal ion–dendrimer loadings. In all cases, 100% of the Cu(II) ions are bound to the dendrimers. When these groups become fully/predominantly protonated at pH = 5.0, no significant binding of Cu(II) is observed. A more complex metal ion uptake behavior is observed at pH = 7.0. The EOB of Cu(II) goes through a series of two distinct binding steps as metal ion–dendrimer loading increases. Because each of these steps involves an initial linear increase in Cu(II) binding followed by a gradual leveling off and a second increase, we have attributed this behavior to the presence of sites with different Cu(II) binding affinity and capacity within the dendrimers.

To gain insight into metal ion coordination with the amine groups of PAMAM dendrimers, we employed EXAFS spectroscopy to probe the structures of aqueous complexes of Cu(II) with G1-NH₂ and G5-NH₂ EDA core PAMAM dendrimers at pH 7.0. Analysis of the EXAFS spectra of the Cu(II) complex with the G5-NH₂ PAMAM dendrimer suggests that the first binding step involves the formation of octahedral complexes in which a Cu(II) central metal ion is coordinated to 2–4 dendrimer tertiary amine groups and 2 axial water molecules. To account for the Cu(II) ions that are not specifically bound to the dendrimers' tertiary amine groups at pH 7.0, we hypothesized that the second binding step involves the formation of octahedral complexes of Cu(II) with water molecules

trapped inside the G_x-NH₂ PAMAM dendrimer. Finally, we combined the results of our experiments with literature data to formulate phenomenological models (Model1 and Model2) of Cu(II) uptake by G_x-NH₂ PAMAM dendrimers in aqueous solutions. At low metal ion–dendrimer loadings, Model1 and Model2 provide a good fit of the measured EOB of Cu(II) for both dendrimers. For the G4-NH₂ PAMAM dendrimer, Model2 also reproduces the increase in the EOB of Cu(II) observed at higher metal ion–dendrimer loadings following the first plateau (Figure 3). However, Model1 fails to capture this trend. Additional experiments and MD simulations are underway to further assess the validity of the proposed two-site model of metal ion uptake by G_x-NH₂ PAMAM dendrimers in aqueous solutions.

Acknowledgment. We thank Ms. Sa'Nia Carasquero (Graduate Student in Chemical Engineering) and Mr. Kwesi Falconer (Graduate Student in Environmental Engineering) of Howard University School of Engineering for their assistance with the proton and metal ion binding experiments. We also thank Dr. Prabal Maiti of the Materials and Process Simulation Center of the Beckman Institute at the California Institute of Technology for providing prior to publication data on the extent of binding of water molecules to EDA core PAMAM dendrimers. Funding for this work was provided by the National Science Foundation (NSF Grant CTS-0086727) and the U.S. Environmental Protection Agency (NCER STAR Grant R829626). Partial funding for this research was also provided by the Department of Energy (Cooperative Agreement EW15254). The EXAFS spectroscopic investigations were carried out at the Stanford Synchrotron Radiation Laboratory, a national user facility operated by Stanford University on behalf of the U.S. Department of Energy, Office of Basic Energy Sciences.

Supporting Information Available: Synthesis and characterization of the dendrimers evaluated in this study and the titration curves of these dendrimers. This material is available free of charge via the Internet at <http://pubs.acs.org>.

LA036108K